TECHNICAL NOTE

Analysis of Spatial Growth Properties in Live Cells

INTRODUCTION

Understanding spatial growth properties provides invaluable insights into cell growth, interactions among cells, and the intricate organization of heterogeneous cell populations within tissues and organs. This data supports applications ranging from monitoring individual colonies during cell growth to more complex endeavors like tissue engineering, where different regions of the tissue may inherently have different properties. Traditionally, achieving high levels of spatial resolution has primarily relied on optical imaging, which often lacks real-time and label-free capabilities. In contrast, current impedance systems offer the advantage of real-time, label-free measurement, albeit with limited spatial resolution for in-depth study of cell growth features.

In this study, we demonstrate our platform's capacity to effectively investigate the morphological and functional attributes of specific spatial features within cell sheets. We achieve this by harnessing the spatial resolution of our impedance read-outs, complemented by image analysis tools. While we emphasize a few spatial features here, it's important to note that this analysis can be seamlessly adapted to extract a wide range of spatial features according to the researcher's specific needs.

TECHNOLOGY

CytoTronics' electronic microplate features a high-density electrode array in each well, offering an exceptional spatial resolution. Our prototype device used for experiments in this note has a spatial resolution of 25 µm, whereas our commercially-available Pixel system has a spatial resolution of 12.5 µm. This capability enables close to single-cell spatial resolution, facilitating comprehensive analysis across the spectrum of functional and morphological measurements.[1] Each pixel effectively monitors the characteristics of adjacent cells, while the platform's temporal resolution allows for real-time tracking of dynamic changes within cell populations.

Furthermore, the platform seamlessly integrates image analysis tools that empower researchers to identify specific spatial features of interest within impedance images. Subsequently, these tools enable the extraction of underlying functional and morphological data associated with the identified spatial features, enhancing the depth and precision of cellular analysis.

RESULTS

Spatial analysis of impedance images

Colony formation is a widely used indicator in clonal selection assays and serves as a hallmark of cell growth. In our study, we examined three functionally diverse cell lines for their tendency to develop colonies: MDA-MB-231,[2] a mesenchymal-like breast cancer cell line; T84, colon carcinoma cells used as a model of intestinal barrier;[3,4] and Calu-3, lung adenocarcinoma cells with an epithelial morphology and the ability to establish tissue barrier.[5]

Figure 1 illustrates how each of these three cell lines exhibit distinct growth characteristics, as depicted in the impedance images. Our analysis of these impedance images allowed us to extract valuable information regarding confluence (i.e., the percentage of electrodes covered by cells), colony count, and colony size. In this analysis, a colony was identified as a distinct group of cells having a minimum diameter of 50 µm.

The three cell lines exhibit different growth behavior even at comparable confluencies. Calu-3 cells tend to form a few large colonies which merge at later timepoints. T84 cells, on the other hand, grow in numerous colonies that steadily increase in size without merging. MDA-MB-231 cells form a few small colonies at early time points, which rapidly grow in number and then merge forming interconnected colonies. This is reflected in an increase in the colony size and decrease in colony number.

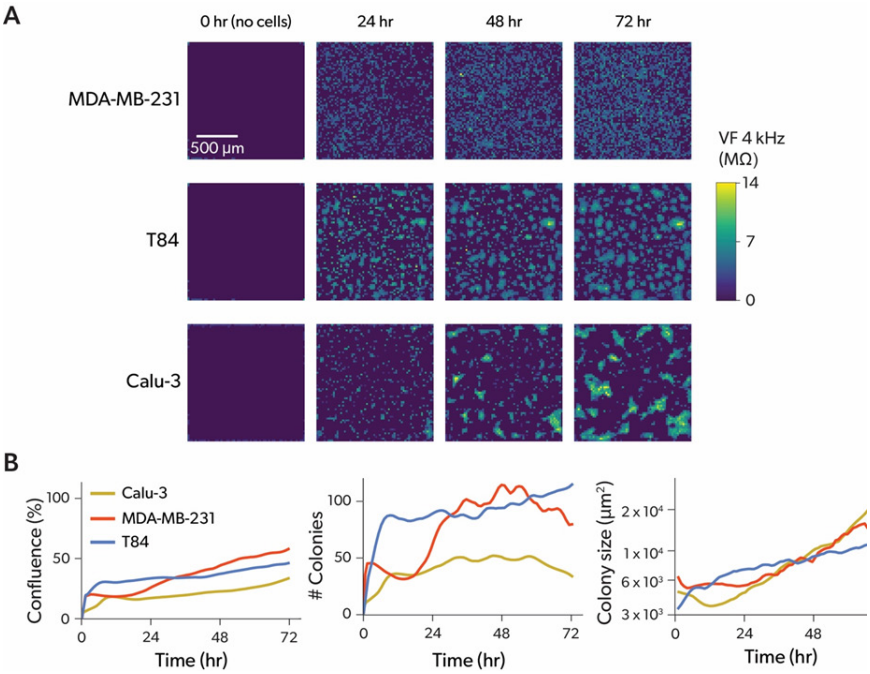

Figure 1. (A) Images for MDA-MB-231, T84 and Calu-3 cells at various times post-seeding. (B) Confluence, average colony number and, average colony size for the three cell lines over 72 hours of growth, calculated from time-series impedance images.

Assessing functional and morphological properties of colonies

Colonies can be further filtered by size, to segregate different populations. In Figure 2, T84 cells were categorized into small colonies (ranging from 50 to 250 µm in diameter) and large colonies (> 250 µm in diameter) over 72 hours of growth. Functional and morphological properties of small and large colonies were then assessed.

As seen in Figure 2B, small colonies have higher surface attachment compared to their larger counterparts. This difference may indicate a shift in cell function once a colony surpasses a certain size threshold.

Interestingly, cell-cell adhesion is initially quite similar in both small and large colonies, but gradually increases in the larger colonies at later time points. This observation suggests that cells in the interior of larger colonies may establish stronger cell-cell connections, contributing to the increase in overall cell-cell adhesion. Spatial analysis unveils novel insights into cell behavior, shedding light on previously unexplored aspects of cell dynamics.

Tracking functional features of a cell sheet over time

Spatial analysis can also be extended beyond colony identification. Figure 3A illustrates the capability to identify cell sheets in Calu-3 and A549 cells and distinguish them from smaller colonies (< 750 µm in diameter) that are not part of the cell sheet. Furthermore, we applied an edge detection algorithm to detect the edges of the growing cell sheet.

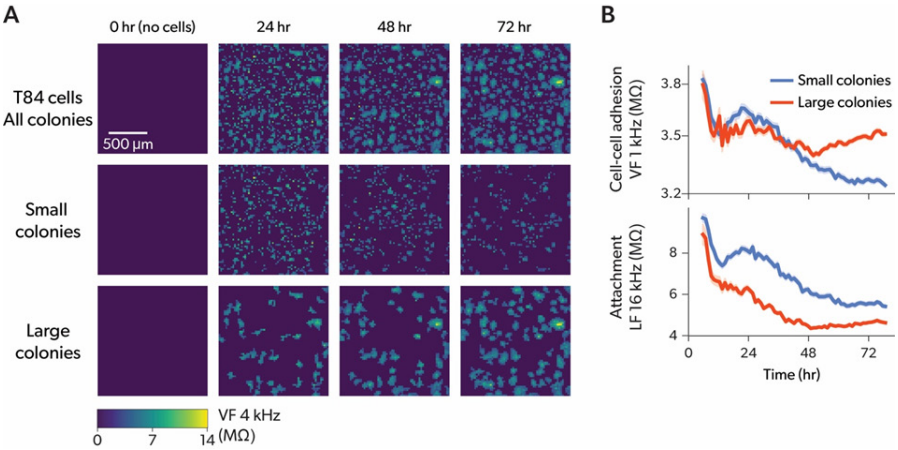

Figure 2. (A) Images of T84 cells at various timepoints during growth. All colonies (top) were then sorted by size to separate small (middle) and large (bottom) colonies. (B) Cell-cell adhesion and attachment for small (blue) and large (orange) colonies plotted over 72 hours of growth.

Calu-3 cells serve as a model for bronchial epithelial barriers, with their tight junctions contributing to a robust tissue barrier.[5] A549 (lung adenocarcinoma)[5] cells are epithelial in nature and do not form strong tight junctions or discernible tissue barriers. We conducted a comparison of sheet edge and center properties between these two cell types.[6] Based on the known behavior of these cell lines, we hypothesized that for Calu-3 cells, the center of the cell sheet, a region with intact cell-cell connections, would exhibit different properties as compared to the leading edge of the cell sheet, where fewer cell-cell connections are formed. For A549 cell, we did not anticipate these differential behaviors.

To test this hypothesis, we tracked the functional properties of the edge and centers of cell sheets over time. As anticipated, in Calu-3 cells, the center of the cell sheet exhibited a significantly higher tissue barrier compared to the edge and this discrepancy intensified over time (Fig. 3B). Similarly, the flatness of cells at the edge remained consistently higher than that at the center. This difference in flatness may be attributed to the central cells becoming more densely packed, growing taller, or differentiating. However, in A549 cells, which do not establish tight cell-cell connections, no discernible distinctions in barrier properties or flatness were observed between the edge and center (Fig. 3B).

To further confirm differential properties across cell sheets, we selected a time point where the cell sheet is sub-confluent with detectable edges (Fig. 4A), and created plots illustrating the tissue barrier as a function of distance from the edge. In the case of Calu-3 cells at 72 hours post seeding, these plots revealed that tissue barrier gradually increases and reaches a maximum value at a distance of 200 µm from the edge (Fig. 4B). On the other hand, flatness initially increases, and then starts to decrease about 100 µm from the edge (Fig. 4B). This analysis can provide detailed information on tissue organization and maturation. Conversely, A549 cells at 48 hours post seeding displayed consistent flatness across their cell sheet, with no substantial variations in barrier properties as a function of distance from the edge (Fig 4B).

This comprehensive analysis underscores the significant differences in cell behavior and properties between the edge and center of cell sheets in Calu-3 and A549 cells, shedding valuable light on the dynamics governing tissue barrier formation.

CONCLUSION

CytoTronics' Pixel platform provides a precise real-time assessment of a range of impedance parameters at high spatial resolution. The platform can measure and visualize functional properties of spatial features of cell sheets through impedance

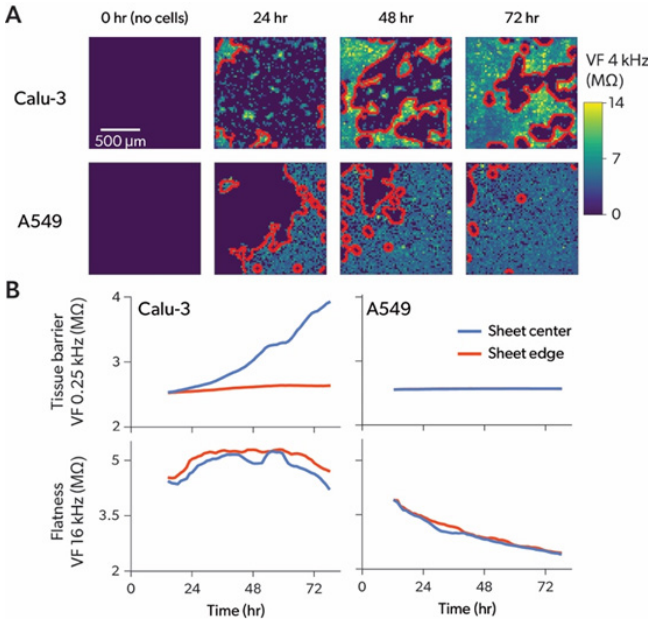

Figure 3. (A) Images of Calu-3 (top) and A549 cells (bottom) at various timepoints during growth, with the sheet edge highlighted in red (bottom). (B) Tissue barrier and attachment of Calu-3 (left) and A549 (right) cells within the sheet (blue) and along the growing edge (orange) plotted over 72 hours of growth.

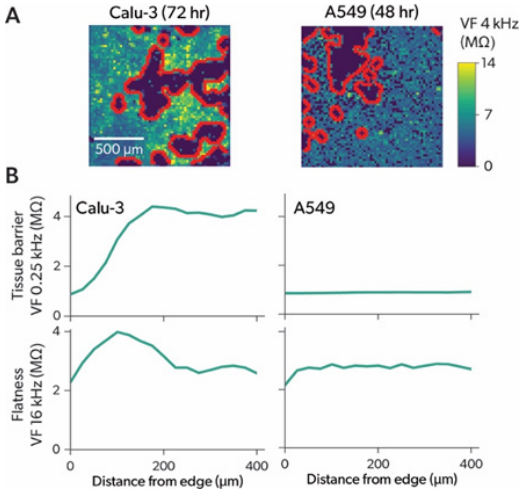

Figure 4. (Images of a sub-confluent cell sheet of Calu-3 and A549 cells at 72 hours and 48 hours post seeding respectively, with edges highlighted in red. (B) Tissue barrier (top) and flatness (bottom) plotted as a function of distance from the growing edges, calculated from the images in A.

images. This spatial resolution offers valuable insights into studying cells with distinct properties, making the platform an invaluable tool for cell analysis.

METHODS

Cell Lines and culture

All cell lines were obtained from ATCC and maintained in a humidified incubator at 37°C and 5% CO_2. MDA-MB-231 (HTB-26), T84 (CCL-248), Calu-3 (HTB-55), and A549 (CCL-185) cells were cultured in DMEM supplemented with 10% FBS and Penicillin-Streptomycin.

Measurements

Impedance measurements were taken at 0.25, 1, 4, and 16 kHz inside a humidified incubator at 37°C and 5% CO_2. Cells were plated at 10,000 – 20,000 cells per well and allowed to grow for up to 72 hours.

Data analysis

Confluence was calculated as a percentage of electrodes occupied by cells. Colonies were identified as group of cells with a minimum diameter of 50 µm separated by at least 25 µm. Colony analysis was performed by first setting size thresholds to filter colonies by their diameter. Sheet analysis was performed by applying a size filter to remove any colonies smaller than a set threshold. An edge detection algorithm was then applied to identify the cells along the edge and isolate the cells away from the edge. For both colony and sheet analysis, impedance values were extracted from the images post filtering. Distance from the sheet edge was calculated for every cell within the sheet from the nearest edge.

REFERENCES

1. Chitale, S. et al. A semiconductor 96-microplate platform for electrical-imaging based high-throughput phenotypic screening. *Nat Commun* **14**, 7576 (2023).
2. Cailleau, R., Young, R., Olivé, M. & Reeves, W. J. Breast tumor cell lines from pleural effusions. *J Natl Cancer Inst* **53**, 661–74 (1974).
3. Brady, R. C., Karnaky, K. J. & Dedman, J. R. Reserpine-induced alterations in mucus production and calmodulin-binding proteins in a human epithelial cell line. *Exp Cell Res* **150**, 141–51 (1984).
4. Dharmsathaphorn, K., McRoberts, J. A., Mandel, K. G., Tisdale, L. D. & Masui, H. A human colonic tumor cell line that maintains vectorial electrolyte transport. *Am J Physiol* **246**, G204-8 (1984).
5. Foster, K. A., Avery, M. L., Yazdanian, M. & Audus, K. L. Characterization of the Calu-3 cell line as a tool to screen pulmonary drug delivery. *Int J Pharm* **208**, 1–11 (2000).
6. Garcia-de-Alba, C. Repurposing A549 Adenocarcinoma Cells: New Options for Drug Discovery. *Am J Respir Cell Mol Biol* **64**, 405–406 (2021).

38 Wareham St, Boston, MA 02118
contact@cytotronics.com
cytotronics.com